

RS-SSM: Refining Forgotten Specifics in State Space Model for Video Semantic Segmentation

Kai Zhu¹, Zhenyu Cui², Zehua Zang^{3,4}, Jiahuan Zhou^{1*}

¹Wangxuan Institute of Computer Technology, Peking University, ²Tsinghua University,

³Institute of Software Chinese Academy of Sciences, ⁴University of Chinese Academy of Sciences

zhukai2022@ruc.edu.cn, cuizhenyu@mail.tsinghua.edu.cn,

zehua2020@iscas.ac.cn, jiahuanzhou@pku.edu.cn

Abstract

Recently, state space models have demonstrated efficient video segmentation through linear-complexity state space compression. However, Video Semantic Segmentation (VSS) requires pixel-level spatiotemporal modeling capabilities to maintain temporal consistency in segmentation of semantic objects. While state space models can preserve common semantic information during state space compression, the fixed-size state space inevitably forgets specific information, which limits the models' capability for pixel-level segmentation. To tackle the above issue, we proposed a **Refining Specifics State Space Model** approach (RS-SSM) for video semantic segmentation, which performs complementary refining of forgotten spatiotemporal specifics. Specifically, a Channel-wise Amplitude Perceptron (CwAP) is designed to extract and align the distribution characteristics of specific information in the state space. Besides, a Forgetting Gate Information Refiner (FGIR) is proposed to adaptively invert and refine the forgetting gate matrix in the state space model based on the specific information distribution. Consequently, our RS-SSM leverages the inverted forgetting gate to complementarily refine the specific information forgotten during state space compression, thereby enhancing the model's capability for spatiotemporal pixel-level segmentation. Extensive experiments on four VSS benchmarks demonstrate that our RS-SSM achieves state-of-the-art performance while maintaining high computational efficiency. The code is available at <https://github.com/zhujiahuan1991/CVPR2026-RS-SSM>.

1. Introduction

Video Semantic Segmentation (VSS) is a fundamental task in the field of computer vision, which aims to assign semantic labels to each pixel in videos and plays a crucial role in understanding the temporal evolution of scenes [10, 20, 21,

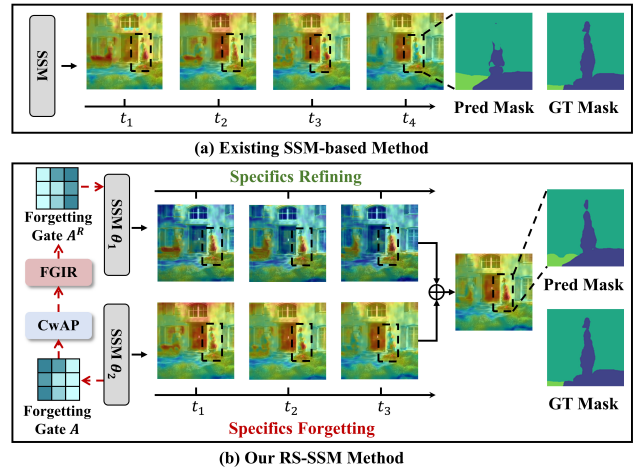


Figure 1. Existing SSM-based VSS methods lose spatiotemporal specifics when perform state space compression, limiting the model's segmentation accuracy. In contrast, our proposed RS-SSM method guides the model to focus on forgotten spatiotemporal specifics, thereby improving the pixel-level semantic segmentation performance.

[50, 51]. With the advancement of deep learning [8, 30, 62–68, 74], VSS has demonstrated extensive practical application potential in areas such as autonomous driving [17], video surveillance [43], and video editing [70]. In complex long videos, objects may undergo significant displacement, deformation, and occlusion, requiring models to maintain temporal consistency in edge segmentation of semantic objects [5, 44], which poses critical challenges to their pixel-level spatiotemporal modeling capabilities.

In the field of VSS, early works utilized optical flow to model pixel-level motion information between adjacent frames, propagating and fusing features from previous frames to aggregate temporal information for segmentation of semantic objects [6, 11, 12, 38, 45]. However, such methods are not only computationally expensive but also suffer from inaccurate and noisy optical flow estimation in long

*Corresponding author

videos with complex object motion, leading to limited video segmentation accuracy. Recent research has focused on using Transformer-based models to aggregate spatiotemporal features [23, 26, 28, 53–55]. These models leverage the global attention mechanism of the Transformer architecture to aggregate information from multiple frames, improving the segmentation accuracy of semantic objects in videos. However, due to the quadratic complexity of their attention computation, these methods face computational and memory bottlenecks when processing long video sequences.

To efficiently aggregate spatiotemporal information in long video sequences, recent research has introduced methods based on State Space Models (SSM) [9, 13, 29]. Leveraging selective gating mechanisms, such methods can efficiently compress and propagate spatiotemporal semantic information with fixed-size state space while achieving competitive semantic segmentation accuracy [22]. Nevertheless, as shown in Figure 1(a), while state space models can preserve common semantic information (e.g., global structure and smooth regions) during state space compression, this fixed-size state space compression process inevitably compromises pixel-level spatiotemporal specifics (e.g., boundaries, textures, local variations), resulting in only coarse segmentation of object locations when performing pixel-level semantic segmentation in videos, but suffering from specifics forgetting. This is detrimental to maintaining temporal consistency of segmentation results for pixel-level semantic information in VSS tasks.

To address the above challenge, we propose a Refining Specifics State Space Model approach, named RS-SSM, which performs complementary refining of the specific information forgotten during the SSM’s state space compression process, thereby overcoming the limitations of existing SSM-based VSS methods. Specifically, considering the differences in information contained across the hidden states of different channels in state space models, we design a Channel-wise Amplitude Perceptron (CwAP) module that computes the information distribution characteristics of different channels in the state space model through frequency domain analysis, obtaining Spectrum Features to quantify the differences in specific information amount across channels. Meanwhile, we introduce a channel information loss that minimizes the differences in normalized Spectrum Features across different samples based on cosine similarity, aiming to align the channel distribution characteristics of specific information across samples and encourage RS-SSM to focus on channels rich in specific information. Leveraging the Spectrum Features extracted by the CwAP module, our designed Forgetting Gate Information Refiner (FGIR) module can adaptively invert and refine the forgetting gate matrix of the SSM, thereby guiding our RS-SSM to focus on refining the specific information forgotten during the state space compression process. As

shown in Figure 1(b), benefiting from the guidance of the CwAP and FGIR modules, RS-SSM forms a supplementary specifics refining process, enhancing the capability to capture specific information while maintaining the ability to model common semantic information, thereby improving the pixel-level segmentation performance in VSS tasks.

To sum up, the main contributions of this work are: (1) We identify the limitation of existing SSM-based VSS methods in modeling spatiotemporal specific information and propose a Refining Specifics State Space Model (RS-SSM) to address this issue. (2) We design a Channel-wise Amplitude Perceptron (CwAP) module to extract channel-wise specific information distribution characteristics, and a Forgetting Gate Information Refiner (FGIR) module to adaptively refine the forgetting gate matrix of the SSM, thereby encouraging RS-SSM to focus on spatiotemporal specific information and improving pixel-level segmentation accuracy. (3) Extensive experiments on multiple VSS benchmarks demonstrate that our RS-SSM achieves superior performance against existing methods.

2. Related Work

2.1. VSS based on CNNs

Among all Convolutional Neural Network (CNN)-based methods, Fully Convolutional Networks (FCN) for natural image semantic segmentation pioneered an end-to-end pixel-level classification framework [47]. However, as video streams represent a more realistic data modality, researchers have increasingly focused on video semantic segmentation tasks, and how to effectively aggregate and propagate spatiotemporal information in video streams has become a key research focus in this field.

Early works combined CNNs [31] with feature propagation based on optical flow estimation and other techniques, leveraging spatiotemporal information to improve segmentation accuracy or reduce computational costs. DFF [77] and Accel [24] propagate features between adjacent frames through optical flow estimation, while GSVNET [27] and EVS [40] reduce computational burden by propagating features from key frames to non-key frames. ClockNet [46] and LLVS [31] introduce adaptive feature reuse, utilizing cross-frame semantic similarity to improve segmentation efficiency and temporal consistency. However, the uncertainty of dynamic scenes makes the aforementioned methods susceptible to cumulative errors, thereby reducing segmentation accuracy. ETC [32] encodes multi-frame dependencies as latent embeddings by introducing the recurrent unit ConvLSTM [49] to leverage temporal information for improved segmentation accuracy. However, the high computational cost and memory requirements of recurrent networks, as well as LSTM’s sensitivity to sequence length [42], limit the scalability of such methods when pro-

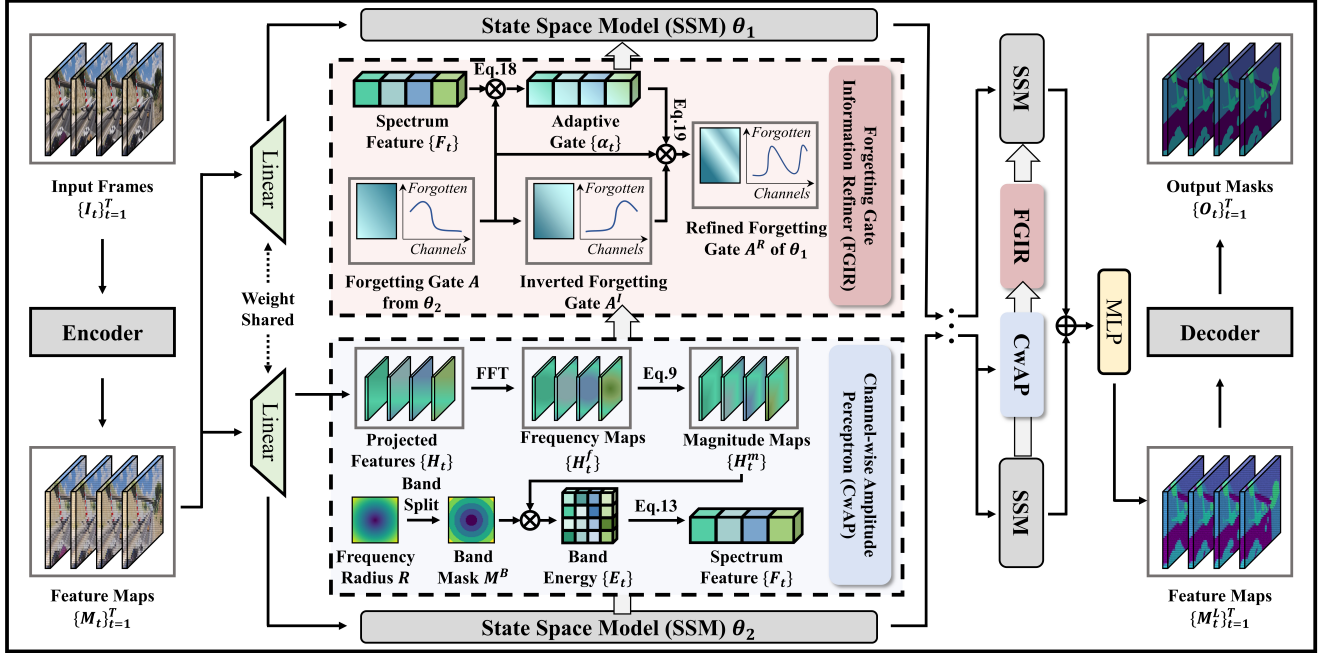


Figure 2. The pipeline of our RS-SSM. Following previous work [22, 61], we use an image encoder to extract feature maps for each frame. After linear projection, we extract spectrum features through the CwAP module to quantify the channel distribution of specific information. Then our FGIR module adaptively inverts and refines the forgetting gate from the SSM θ_2 , thereby encouraging SSM θ_1 to perform complementary refining of forgotten spatiotemporal specifics.

cessing long video sequences.

2.2. VSS based on Transformers

Inspired by the success of Transformer models in natural language processing [56], recent researchers have shifted toward using Transformer architectures in VSS to better capture long-range spatiotemporal dependencies in videos [69]. TDNet [23] uses attention modules to aggregate and propagate features from consecutive frames, while STT [28] and LMANet [41] extract features from reference frames through attention mechanisms to assist in segmenting target frames. MPVSS [59] achieves efficient temporal aggregation for longer video sequences through a memory-augmented Transformer framework. Similarly, CFFM [53] and MRCFA [54] employ multi-resolution inter-frame attention mechanisms to handle temporal variations through intra-frame contextual static-dynamic decoupling, thereby achieving pixel-level segmentation processes that distinguish between stationary and moving elements.

Although Transformer-based VSS models have achieved significant progress, the quadratic complexity of their attention mechanism results in high computational costs and memory requirements when processing high-resolution frames or long video sequences [25, 48, 58]. This challenge highlights the need for next-generation VSS model architectures that can effectively model long-range spatiotemporal

information while improving computational efficiency.

2.3. State Space Models

In recent years, State Space Models (SSMs) have emerged as a promising approach for sequence modeling [16, 18]. Through HiPPO initialization [14, 15], SSMs possess the ability to capture long-range dependencies with linear computational complexity. Building on this foundation, Mamba and Mamba2 introduced input-dependent update and forget gates to address limitations in content-based reasoning [9, 13]. Unlike Transformer architectures, this allows SSM parameters to be dynamically modulated by input, significantly improving expressiveness in discrete modalities. Coupled with hardware-friendly parallelization, these advances lead to notable gains in computational efficiency and performance in language modeling [57, 72, 78].

Building on this progress, recent work has introduced SSMs into the vision domain [19, 29, 33, 36, 39, 60, 71, 73, 75, 76]. Vision Mamba extends the Mamba framework to 2D image modeling through bidirectional spatial scanning [33, 76], while U-Mamba combines SSMs with convolutional layers, achieving superior performance in medical image segmentation tasks [36]. VideoMamba further introduces spatiotemporal scanning, becoming a competitive backbone network in video domain [2, 29, 35, 39]. TV3S is the first to apply SSMs to video semantic seg-

mentation tasks, achieving efficient information propagation in long video sequences [22]. However, existing SSM-based VSS methods often overlook the rich spatiotemporal specifics in videos during state space compression, which limits the pixel-level segmentation accuracy of such methods in videos. To this end, our proposed RS-SSM effectively refines the forgotten specifics, achieving superior segmentation performance.

3. Method

In this section, we illustrate the proposed RS-SSM comprehensively, and the overall pipeline is depicted in Figure 2.

3.1. Preliminary

The SSM-based models are inspired by continuous systems that map one-dimensional functions $x(t) \in \mathbb{R} \mapsto y(t) \in \mathbb{R}$ through a hidden state $h(t) \in \mathbb{R}^{D_s}$, where the state space is D_s -dimensional.

For multi-channel token processing, the model maintains D independent SSMs, where each channel $d \in \{1, \dots, D\}$ has its own D_s -dimensional state space. To reduce computational complexity, the state evolution matrix is diagonalized. For a single channel d , the hidden state evolves as follows:

$$h'_d(t) = \mathbf{A}_d \odot h_d(t) + \mathbf{B}_d x_d(t), \quad y_d(t) = \mathbf{C}_d^\top h_d(t), \quad (1)$$

where $\mathbf{A}_d \in \mathbb{R}^{D_s}$ is the diagonal forgetting vector for channel d , $\mathbf{B}_d \in \mathbb{R}^{D_s}$ denotes the update vector, $\mathbf{C}_d \in \mathbb{R}^{D_s}$ serves as the output projection vector, and \odot represents element-wise multiplication. Across all channels, the forgetting vector forms a forgetting gate matrix $\mathbf{A} \in \mathbb{R}^{D \times D_s}$.

To facilitate application in deep learning, SSMs are discretized into discrete-time systems. For each channel, the continuous parameters are transformed using a learnable time step $\Delta_d \in \mathbb{R}$:

$$\begin{aligned} \bar{\mathbf{A}}_d &= \exp(\Delta_d \mathbf{A}_d), \\ \bar{\mathbf{B}}_d &= (\Delta_d \mathbf{A}_d)^{-1} \odot (\exp(\Delta_d \mathbf{A}_d) - \mathbf{1}) \odot (\Delta_d \mathbf{B}_d), \end{aligned} \quad (2)$$

where operations are element-wise. The discretized SSM for channel d is:

$$h_{d,t} = \bar{\mathbf{A}}_d \odot h_{d,t-1} + \bar{\mathbf{B}}_d x_{d,t}, \quad y_{d,t} = \mathbf{C}_d^\top h_{d,t}, \quad (3)$$

where $h_{d,t-1}, h_{d,t} \in \mathbb{R}^{D_s}$, and $x_{d,t}, y_{d,t} \in \mathbb{R}$. For a complete token at time t , we have $\mathbf{x}_t = [x_{1,t}, \dots, x_{D,t}]^\top \in \mathbb{R}^D$ and $\mathbf{y}_t = [y_{1,t}, \dots, y_{D,t}]^\top \in \mathbb{R}^D$.

The discretized evolution parameters $\bar{\mathbf{A}}_d = \exp(\Delta_d \mathbf{A}_d)$ act as element-wise decay factors that govern the degree of information compression from previous hidden states. Since \mathbf{A}_d is constrained to be negative, each element of $\bar{\mathbf{A}}_d$ lies in $(0, 1)$, where smaller values impose more aggressive state space compression on historical information

in $h_{d,t-1}$, while values closer to 1 preserve more information with minimal state space compression.

3.2. Overall Architecture

Our RS-SSM architecture processes input video frames $\{I_t\}_{t=1}^T$, where T is the number of frames. An image encoder $\mathcal{E}(\cdot)$ extracts feature maps $\{M_t\}_{t=1}^T$ from each frame:

$$M_t = \mathcal{E}(I_t), \quad t \in \{1, \dots, T\}. \quad (4)$$

Each feature map $M_t \in \mathbb{R}^{C \times H \times W}$ has channel dimension C , height H and width W . After the image encoder, we stack L dual-path SSM layers, and each layer contains two SSM modules $\theta_1^l, \theta_2^l, l \in \{1, \dots, L\}$. For the input to the l -th dual-path layer, we denote it as M_t^{l-1} . Within each dual-path SSM layer, the input feature map is first mapped to a D -dimensional projected feature through a weight-shared linear projection $\mathcal{P}(\cdot)$:

$$H_t^{l-1} = \mathcal{P}(M_t^{l-1}), \quad t \in \{1, \dots, T\}, \quad (5)$$

where $H_t^{l-1} \in \mathbb{R}^{D \times H \times W}$. Subsequently, the projected features $\{H_t^{l-1}\}_{t=1}^T$ are fed into the SSM modules for spatiotemporal modeling, respectively. These outputs are concatenated along the channel dimension and then fused through an MLP layer to obtain the output feature map of the l -th layer:

$$M_t^l = \text{MLP}(\text{Concat}[\theta_1^l(H_t^{l-1}), \theta_2^l(H_t^{l-1})]), \quad (6)$$

where $t \in \{1, \dots, T\}$. Finally, after passing through all L dual-path SSM layers, the output feature maps $\{M_t^L\}_{t=1}^T$ are fed into a linear segmentation decoder \mathcal{D} to generate the final segmentation masks for each frame:

$$O_t = \mathcal{D}(M_t^L), \quad t \in \{1, \dots, T\}. \quad (7)$$

3.3. Channel-wise Amplitude Perceptron (CwAP)

As mentioned in Sec 1, the CwAP module computes the information distribution characteristics of different channels in the projected features $\{H_t\}_{t=1}^T$, where $H_t \in \mathbb{R}^{D \times H \times W}$. Following previous works [3, 4], we employ frequency domain transformation to quantify the amount of specific information in different channels. For each projected feature H_t , we first apply 2D Fast Fourier Transform to convert it into the frequency domain:

$$H_t^f = \text{FFT2D}(H_t) \in \mathbb{C}^{D \times H \times W}. \quad (8)$$

To extract the energy distribution information in the frequency domain and thereby quantify the energy proportion across different frequency bands, we compute the magnitude map as follows:

$$H_t^m = \sqrt{(\text{Re}(H_t^f))^2 + (\text{Im}(H_t^f))^2} \in \mathbb{R}^{D \times H \times W}, \quad (9)$$

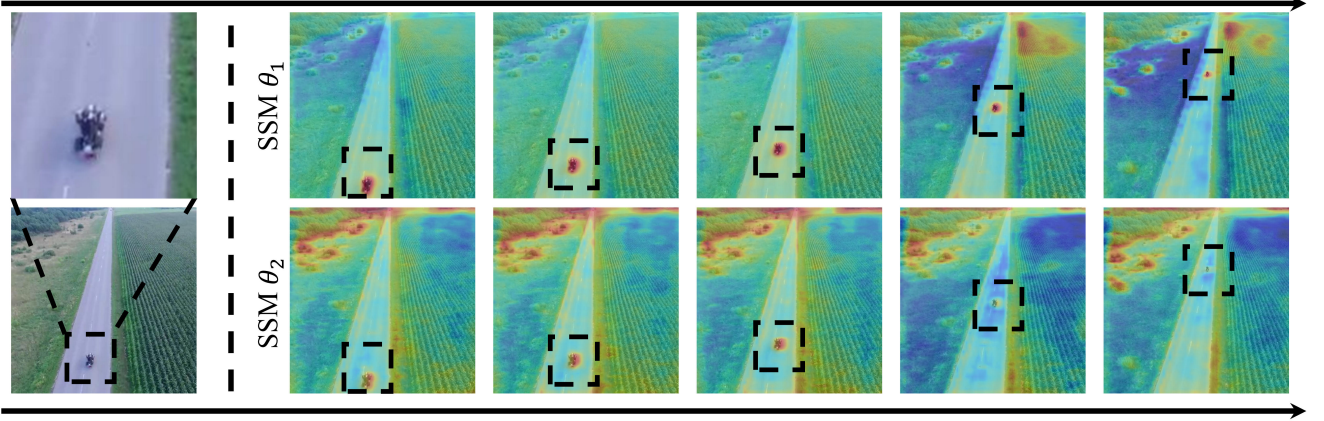


Figure 3. Visualization of the updating gate $\overline{\mathbf{B}}_d$ as mentioned in Eq 2. Influenced by the forgetting gate, the updating gate reflects the amount of new information introduced at each time step. The bottom row visualization reveals that the vanilla SSM θ_2 suffers from information loss of specifics during the state space compression. Conversely, as illustrated in the top row, the SSM θ_1 effectively refines these forgotten specifics after inverting and refining the forgetting gate.

where $\text{Re}(\cdot)$ and $\text{Im}(\cdot)$ denote the real and imaginary parts, respectively. We partition the frequency domain into K bands based on normalized frequency radius, where low-frequency bands correspond to common semantic information (e.g., global structure, smooth regions) and high-frequency bands correspond to specific information (e.g., boundaries, textures, local variations):

$$R_t(h, w) = \sqrt{\left(\frac{h - H/2}{H}\right)^2 + \left(\frac{w - W/2}{W}\right)^2}, \quad (10)$$

where we center the frequency spectrum. For the k -th frequency band $k \in \{0, 1, \dots, K-1\}$, we define the binary band mask:

$$M_{t,k}^b = 1 \left\{ \frac{k}{K} \leq R_t(h, w) < \frac{k+1}{K} \right\}, \quad (11)$$

where $1\{\cdot\}$ is the indicator function that outputs 1 if the condition is satisfied and 0 otherwise. The energy in band k for each channel is:

$$E_{t,c,k} = \sum_{h,w} H_{t,c,h,w}^m \cdot M_{t,k}^b(h, w). \quad (12)$$

The energy distribution is normalized to obtain a probability distribution, and the spectrum features $F_t \in \mathbb{R}^C$ is computed as the cumulative energy ratio from the top- k_h high-frequency bands:

$$\tilde{E}_{t,c,k} = \frac{E_{t,c,k}}{\sum_{k'=0}^{K-1} E_{t,c,k'}}, \quad F_{t,c} = \sum_{k=K-k_h}^{K-1} \tilde{E}_{t,c,k}, \quad (13)$$

where k_h denotes the number of high-frequency bands used for specifics distribution measurement. The obtained spectrum features F_t reflect the amount of specific information

in each channel and will be used to guide the subsequent forgetting gate invert and refinement in the FGIR module.

To promote consistency in subsequent specifics refining, we aim to align the channel distribution of specific information across samples, i.e., guide the specific information in different samples to be distributed in similar channels. Specifically, we normalize the features and compute cosine similarity between all pairs, obtaining the similarity matrix for frame batch $\mathcal{B} = \{1, 2, \dots, B \cdot T\}$:

$$\hat{F} = \frac{F}{\|F\|_2}, \quad \mathbf{S}_{i,j} = \hat{F}_i^\top \hat{F}_j, \quad \forall i, j \in \mathcal{B}, \quad (14)$$

where B is the batch size of videos, and T is the number of sampled frames per video.

We introduce a channel information loss \mathcal{L}_{ci} to maximize the average pairwise cosine similarity in the batch, defined as:

$$\mathcal{L}_{\text{ci}} = 1 - \frac{1}{|\mathcal{B}|^2} \sum_{i=1}^{|\mathcal{B}|} \sum_{j=1}^{|\mathcal{B}|} \mathbf{S}_{i,j}. \quad (15)$$

By minimizing this loss, the model learns to allocate specific information to the same subset of channels. This consistency allows the subsequent FGIR module to selectively enhance these specifics-rich channels, thereby promoting the effectiveness of specifics refining.

3.4. Forgetting Gate Information Refiner (FGIR)

As mentioned in Sec 3.1, the forgetting gate matrix $\mathbf{A} \in \mathbb{R}^{D \times D_s}$ in SSMs controls the degree of information compression from previous hidden states. In our RS-SSM, we propose the FGIR module to adaptively invert and refine the forgetting gate from the SSM θ_2^l based on the spectrum features $\{F_i\}_{i=1}^{B \cdot T}$ extracted by the CwAP module, and then

Table 1. The comparison with existing methods on the VSPW [37], NYUv2 [52] and CamVid [1] dataset. Our RS-SSM achieves state-of-the-art performance while maintaining high efficiency. The best and second-best results are highlighted in **RED** and **BLUE**, respectively. We calculate GFLOPs and FPS with an input resolution of 480×853 .

Methods	Backbones	mIoU \uparrow			GFLOPs \downarrow	Params(M) \downarrow	FPS \uparrow
		VSPW	NYUv2	CamVid			
Segformer [61]	MiT-B1	36.5	37.6	57.9	26.6	13.8	58.7
CFFM++ [55]	MiT-B1	39.9	39.5	60.1	114.3	16.5	27.6
MRCFA [54]	MiT-B1	38.9	39.1	59.7	77.5	16.2	40.1
TV3S [22]	MiT-B1	40.0	39.7	60.8	36.9	17.3	24.7
RS-SSM (Ours)	MiT-B1	41.7	41.4	62.7	48.1	20.2	37.3
Segformer [61]	MiT-B2	43.9	42.1	59.8	100.8	24.8	16.2
CFFM++ [55]	MiT-B2	45.5	43.9	61.0	172.6	28.5	21.5
MRCFA [54]	MiT-B2	45.3	43.5	60.6	127.9	27.3	10.7
TV3S [22]	MiT-B2	46.3	44.7	61.8	53.9	28.3	21.9
RS-SSM (Ours)	MiT-B2	46.8	45.9	63.7	60.7	31.2	30.9
Mask2Former [5]	R50	38.5	41.7	58.1	110.6	44.0	19.4
MPVSS [59]	R50	37.5	40.1	59.7	38.9	84.1	33.9
Mask2Former [5]	R101	39.3	41.3	58.9	141.3	63.0	16.9
MPVSS [59]	R101	38.8	40.4	58.8	45.1	103.1	32.3
Segformer [61]	MiT-B5	48.9	46.1	61.4	185.0	82.1	9.4
CFFM++ [55]	MiT-B5	50.1	46.7	62.3	444.3	87.5	10.4
MRCFA [54]	MiT-B5	49.9	46.7	61.8	373.0	84.5	5.0
TV3S [22]	MiT-B5	49.8	46.9	62.1	137.0	85.6	14.0
RS-SSM (Ours)	MiT-B5	51.6	49.1	64.4	128.8	88.4	20.2
Mask2Former [5]	Swin-T	41.2	37.4	58.7	114.4	47.4	17.1
MPVSS [59]	Swin-T	39.9	36.8	58.3	39.7	114.0	32.8
TV3S [22]	Swin-T	44.9	40.5	59.4	57.3	31.7	22.9
RS-SSM (Ours)	Swin-T	46.1	42.2	60.9	73.5	34.6	26.7
Mask2Former [5]	Swin-S	42.1	43.1	59.6	152.2	68.9	14.5
MPVSS [59]	Swin-S	40.4	41.7	59.3	47.3	108.0	30.6
TV3S [22]	Swin-S	50.6	45.2	60.2	94.1	53.1	19.5
RS-SSM (Ours)	Swin-S	52.2	47.0	62.0	110.3	55.9	24.2

feed the refined forgetting gate into the SSM θ_1^l as its parameter matrix. This encourages RS-SSM to perform complementary refining of specific information.

Given the forgetting gate matrix \mathbf{A} in the SSM θ_2^l , we first compute the inverted version of \mathbf{A} by inverting its value range along the channel dimension:

$$\mathbf{A}^I = \mathbf{A}_{\max} + \mathbf{A}_{\min} - \mathbf{A} \in \mathbb{R}^{D \times D_s}, \quad (16)$$

where \mathbf{A}_{\max} and \mathbf{A}_{\min} are the maximum and minimum values of \mathbf{A} along the channel dimension, respectively. This operation inverts the compression degree of the forgetting gate across different channels, making originally highly compressed channels less compressed after inversion, and vice versa.

To quantify the compression degree for different channels in the SSM θ_2^l , we compute the importance of each channel from \mathbf{A} :

$$\beta_i = \frac{\|\exp((\mathbf{A})_i)\|_2}{\max_j \|\exp((\mathbf{A})_j)\|_2 + \epsilon}, \quad i = 1, \dots, D, \quad (17)$$

where $\beta \in \mathbb{R}^D$ represents the normalized channel importance, and ϵ is a small constant for the numerical stability.

Channels with higher β_i values are less compressed in the SSM θ_2^l and thus deemed more important.

The inverting weight α is computed based on both the spectrum features and channel importance:

$$\begin{aligned} \tilde{F} &= \text{Softmax}\left(\frac{1}{B \cdot T} \sum_{i=1}^{B \cdot T} F_i\right) \in \mathbb{R}^D, \\ \alpha &= \tilde{F} \odot (1 - \beta) \in \mathbb{R}^D, \end{aligned} \quad (18)$$

where \odot denotes element-wise multiplication. Channels with high specific content (\tilde{F}) and low importance ($1 - \beta$) in the SSM θ_2^l receive higher inverting weights.

Finally, we obtained the refined forgetting gate \mathbf{A}^R through adaptive interpolation:

$$\mathbf{A}^R = (1 - \alpha) \odot \mathbf{A} + \alpha \odot \mathbf{A}^I, \quad (19)$$

where \mathbf{A}^R serves as the forgetting gate in the SSM θ_1^l . By inverting and refining the forgetting gate from the SSM θ_2^l , we encourage θ_1^l to focus on complementarily refining specific information that is forgotten by θ_2^l , as shown in Fig 3, thereby enhancing the overall representation capability of our RS-SSM.

Table 2. The comparison with existing methods on the Cityscapes [7] dataset, using an input size of 512×1024 .

Methods	Backbones	mIoU \uparrow	GFLOPs \downarrow	Params(M) \downarrow	FPS \uparrow
SegFormer [61]	MiT-B0	71.9	54.6	3.7	58.5
CFFM [53]	MiT-B0	74.0	80.7	4.6	15.8
MRCFA [54]	MiT-B0	72.8	77.5	4.2	16.6
SegFormer [61]	MiT-B1	74.1	106.4	13.7	46.8
CFFM++ [55]	MiT-B1	75.7	169.8	15.9	20.4
MRCFA [54]	MiT-B1	75.1	145.0	14.9	13.0
TV3S [22]	MiT-B1	75.6	83.6	17.3	25.1
RS-SSM (Ours)	MiT-B1	78.3	59.5	20.1	27.2

Table 3. Ablation study on the influence of different components in our RS-SSM. V-SSM represents only using one vanilla State Space Model path, Bi-V-SSM represents using two-way vanilla State Space Model paths, and No-CwAP using our RS-SSM with a simply inverted forgetting gate as mentioned in Eq 16.

Methods	mIoU \uparrow				
	MiT-B1	MiT-B2	MiT-B5	Swin-T	Swin-S
V-SSM	38.8	45.1	48.5	43.3	49.8
Bi-V-SSM	39.6	45.4	49.0	43.7	50.8
No-CwAP	40.7	46.0	50.2	44.9	51.6
RS-SSM	41.7	46.8	51.6	45.7	52.2

3.5. Overall Optimization

Following previous SSM-based VSS works [22], we employ the standard cross-entropy loss \mathcal{L}_{ce} for supervision. Additionally, we incorporate the channel information loss \mathcal{L}_{ci} from the CwAP module to promote a consistent distribution of specific information across samples. The overall loss function is defined as:

$$\mathcal{L} = \mathcal{L}_{ce}(O_T, Y_T) + \lambda \sum_{t=1}^T \mathcal{L}_{ce}(O_t, Y_t) + \lambda_i \mathcal{L}_{ci}, \quad (20)$$

where Y_t is the ground-truth segmentation mask for frame t . λ and λ_i are hyperparameters that balance the contributions of different loss terms.

4. Experiment

4.1. Datasets and Evaluation Metrics

The experiments are conducted on four VSS datasets: VSPW [37], NYUv2 [52], CamVid [1] and Cityscapes [7]. The largest VSPW [37] dataset contains 3536 video sequences and covers various scenarios, with 2806 sequences for training, 343 for validation, and 387 for testing, including 124 classes. The NYUv2 [52] dataset consists of 1449 video sequences captured in indoor environments, with 795 sequences for training and 654 for testing, annotated with 40 classes. The CamVid [1] dataset contains 701 video sequences recorded in urban driving scenarios, with 369 se-

quences for training, 100 for validation, and 232 for testing, annotated with 32 classes. The Cityscapes [7] dataset comprises 5000 video sequences captured in urban street scenes, with 2975 sequences for training, 500 for validation and 1525 for testing, annotated with 19 classes.

We use the mean Intersection over Union (mIoU) as the evaluation metric for all datasets. To verify the efficiency of our proposed method, we also report the number of parameters (Params), floating point operations (GFLOPs) and inference speed (FPS) during evaluation.

4.2. Implementation details

Our proposed approach is implemented based on MMSegmentation framework and all the experiments were conducted with 4 RTX4090 NVIDIA GPUs. Following the SegFormer [61], we utilize MiT and Swin-Transformer [34] as our backbones, which are pre-trained with ImageNet. For fair comparison, we maintain consistency with previous SSM-based VSS methods [22] by using only the current frame T and frames $T - 9$, $T - 6$, and $T - 3$ as input during the training phase on the VSPW [37] dataset. And the input embedding dimension is set to 256. Frame inputs for the VSPW [37] and the CamVid [1] dataset are cropped to 480×480 , while for NYUv2 [52] and Cityscapes [7] datasets, frames are cropped to 480×640 and 512×1024 , respectively. During training, we use the AdamW optimizer with an initial learning rate of 6×10^{-5} and a weight decay of 0.01. The learning rate is adjusted using the poly learning rate policy with a power of 1.0. Following the prior works, standard data augmentation techniques such as cropping and flipping are applied during training.

4.3. Comparison with State-of-the-arts

We compare our proposed RS-SSM with several state-of-the-art VSS methods on VSPW [37], NYUv2 [52], and CamVid [1], as shown in Tab 1. Among existing methods, TV3S [22] is currently the best SSM-based video semantic segmentation method. We divide the tables into multiple groups based on different backbone types or scales. When using Swin-S and MiT-B5 as backbones, our method surpasses the current state-of-the-art by **1.6** and **1.5** mIoU on the large-scale VSPW dataset, respectively, while maintaining efficient inference speed. This is because our RS-SSM design can effectively capture spatiotemporal specifics in videos with linear complexity, enhancing the model’s pixel-level segmentation capability for semantic objects, as shown in Fig 4. When using smaller-scale backbones such as MiT-B1 and Swin-T, our method also outperforms the current state-of-the-art TV3S [22] by **1.7** and **1.2** mIoU on the VSPW dataset, respectively. Even when constrained by small-scale backbones, our RS-SSM still demonstrates effective performance improvement.

On the smaller-scale datasets NYUv2 and CamVid, our

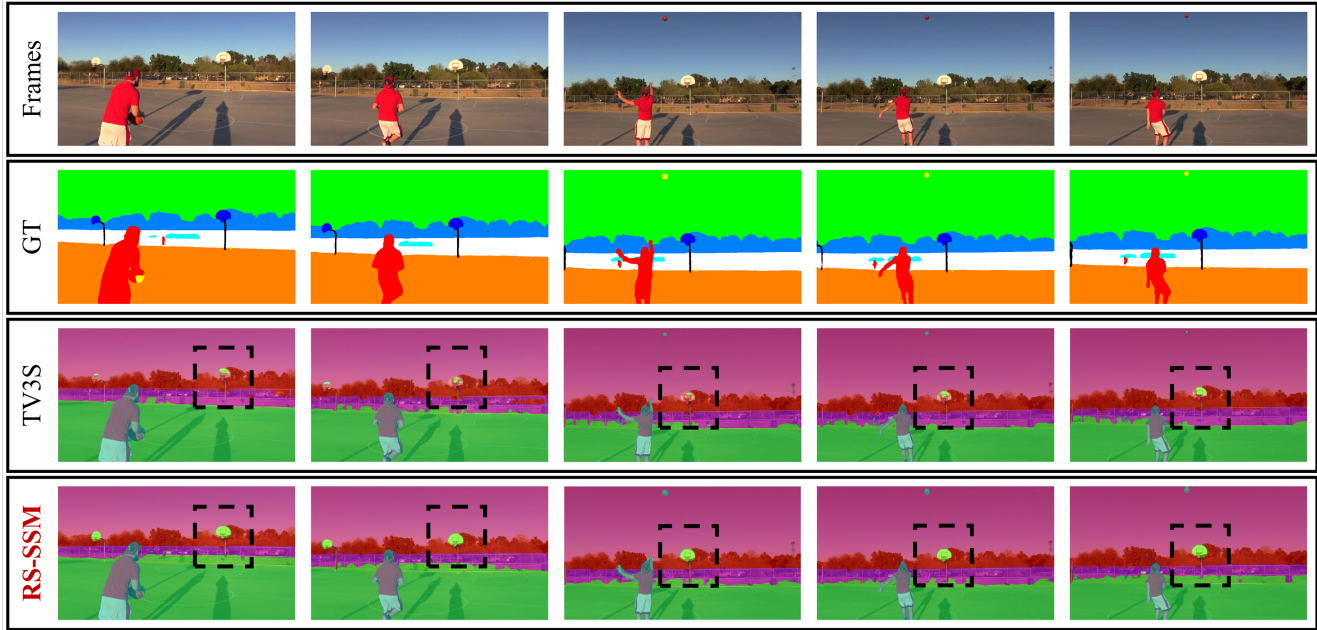


Figure 4. Visualization of segmentation results on VSPW dataset [37]. Compared to the existing SSM-based method TV3S [22], our RS-SSM produces more accurate and detailed segmentation results by effectively refining specific information in videos.

method also achieves significant improvements over existing approaches. When using MiT-B5 as the backbone, our method outperforms the current SSM-based VSS method TV3S [22] by **2.2** mIoU on the NYUv2 dataset and surpasses the state-of-the-art method CFFM++ [55] by **2.1** mIoU on the CamVid dataset. These results further demonstrate the superior capability of RS-SSM for pixel-level semantic segmentation tasks.

We also evaluate our RS-SSM on the **Cityscapes** [7] dataset, as shown in Tab 2. When using MiT-B1 as the backbone, our method surpasses the current state-of-the-art by **2.6** mIoU, demonstrating the effectiveness of RS-SSM in refining spatiotemporal specifics for pixel-level segmentation tasks. This further validates the generalization capability of our RS-SSM across different datasets and scenarios.

Notably, our method not only achieves superior segmentation performance but also exhibits high computational efficiency. As illustrated in Tab 1, when employing MiT-B5 as the backbone, our method reduces GFLOPs by **8.2** and improves FPS by **6.2** compared to the existing SSM-based VSS method TV3S [22] with an input resolution of 480×853 . As shown in Tab 2, when processing input frames of size 512×1024 pixels with MiT-B1 as the backbone, our method achieves a reduction of **24.1** in GFLOPs and an improvement of **2.1** in FPS compared to TV3S [22]. This efficiency gain stems from the design where the linear projection mentioned in Eq 5 is weight-shared and the modules CwAP and FGIR are lightweight, thus preserving the computational efficiency inherent to SSM-based VSS methods.

4.4. Ablation

To validate the effectiveness of different components in our RS-SSM, we conduct ablation studies on the VSPW dataset, as shown in Tab 3. When using only one or two-way vanilla State Space Model (V-SSM and Bi-V-SSM), the performance decreases by up to **3.1** and **2.6** mIoU respectively, demonstrating the importance of modeling specific information. When using RS-SSM with a simply inverted forgetting gate (No-CwAP) in Eq 16, the performance decreases by up to **1.4** mIoU compared to our full RS-SSM. This indicates that the adaptive refinement of the forgetting gate through CwAP is crucial for effectively capturing complementary specific information, thereby enhancing the overall representation capability of our RS-SSM.

5. Conclusion

In this paper, we propose a novel Refining Specifics State Space Model (RS-SSM) for video semantic segmentation. Specifically, we design a Channel-wise Amplitude Perceptron (CwAP) module to extract specific information distribution characteristics and align them in the channel-wise from the state space, as well as Forgetting Gate Information Refiner (FGIR) module to adaptively refine the forgetting gate for better refining complementary spatiotemporal specifics. This approach enhances the model’s ability to capture pixel-level semantic specifics in videos while maintaining computational efficiency. The effectiveness of our proposed RS-SSM has been validated on four datasets for video semantic segmentation.

6. Acknowledgements

This work is a research achievement of the National Engineering Research Center of New Electronic Publishing Technologies, supported by the National Natural Science Foundation of China (62376011) and the National Key R&D Program of China (2024YFA1410000).

References

- [1] Gabriel J Brostow, Jamie Shotton, Julien Fauqueur, and Roberto Cipolla. Segmentation and recognition using structure from motion point clouds. In *European conference on computer vision*, pages 44–57. Springer, 2008. 6, 7
- [2] Guo Chen, Yifei Huang, Jilan Xu, Baoqi Pei, Zhe Chen, Zhiqi Li, Jiahao Wang, Kunchang Li, Tong Lu, and Limin Wang. Video mamba suite: State space model as a versatile alternative for video understanding. *arXiv preprint arXiv:2403.09626*, 2024. 3
- [3] Linwei Chen, Ying Fu, Lin Gu, Chenggang Yan, Tatsuya Harada, and Gao Huang. Frequency-aware feature fusion for dense image prediction. *IEEE transactions on pattern analysis and machine intelligence*, 2024. 4
- [4] Linwei Chen, Lin Gu, and Ying Fu. Frequency-dynamic attention modulation for dense prediction. In *Proceedings of the IEEE/CVF International Conference on Computer Vision*, pages 22620–22632, 2025. 4
- [5] Bowen Cheng, Ishan Misra, Alexander G Schwing, Alexander Kirillov, and Rohit Girdhar. Masked-attention mask transformer for universal image segmentation. In *Proceedings of the IEEE/CVF conference on computer vision and pattern recognition*, pages 1290–1299, 2022. 1, 6
- [6] Jingchun Cheng, Yi-Hsuan Tsai, Shengjin Wang, and Ming-Hsuan Yang. Segflow: Joint learning for video object segmentation and optical flow. In *Proceedings of the IEEE international conference on computer vision*, pages 686–695, 2017. 1
- [7] Marius Cordts, Mohamed Omran, Sebastian Ramos, Timo Rehfeld, Markus Enzweiler, Rodrigo Benenson, Uwe Franke, Stefan Roth, and Bernt Schiele. The cityscapes dataset for semantic urban scene understanding. In *Proceedings of the IEEE conference on computer vision and pattern recognition*, pages 3213–3223, 2016. 7, 8
- [8] Zhenyu Cui, Jiahuan Zhou, Xun Wang, Manyu Zhu, and Yuxin Peng. Learning continual compatible representation for re-indexing free lifelong person re-identification. In *Proceedings of the IEEE/CVF Conference on Computer Vision and Pattern Recognition*, pages 16614–16623, 2024. 1
- [9] Tri Dao and Albert Gu. Transformers are SSMS: Generalized models and efficient algorithms through structured state space duality. In *International Conference on Machine Learning (ICML)*, 2024. 2, 3
- [10] Henghui Ding, Xudong Jiang, Ai Qun Liu, Nadia Magnenat Thalmann, and Gang Wang. Boundary-aware feature propagation for scene segmentation. In *Proceedings of the IEEE/CVF international conference on computer vision*, pages 6819–6829, 2019. 1
- [11] Mingyu Ding, Zhe Wang, Bolei Zhou, Jianping Shi, Zhiwu Lu, and Ping Luo. Every frame counts: Joint learning of video segmentation and optical flow. In *Proceedings of the AAAI conference on artificial intelligence*, pages 10713–10720, 2020. 1
- [12] Yuan Gao, Zilei Wang, Jiafan Zhuang, Yixin Zhang, and Junjie Li. Exploit domain-robust optical flow in domain adaptive video semantic segmentation. In *Proceedings of the AAAI Conference on Artificial Intelligence*, pages 641–649, 2023. 1
- [13] Albert Gu and Tri Dao. Mamba: Linear-time sequence modeling with selective state spaces. *arXiv preprint arXiv:2312.00752*, 2023. 2, 3
- [14] Albert Gu, Tri Dao, Stefano Ermon, Atri Rudra, and Christopher Ré. Hippo: Recurrent memory with optimal polynomial projections. *Advances in neural information processing systems*, 33:1474–1487, 2020. 3
- [15] Albert Gu, Karan Goel, Ankit Gupta, and Christopher Ré. On the parameterization and initialization of diagonal state space models. *Advances in Neural Information Processing Systems*, 35:35971–35983, 2022. 3
- [16] Albert Gu, Karan Goel, and Christopher Ré. Efficiently modeling long sequences with structured state spaces. In *The International Conference on Learning Representations (ICLR)*, 2022. 3
- [17] Diandian Guo, Deng-Ping Fan, Tongyu Lu, Christos Sakaridis, and Luc Van Gool. Vanishing-point-guided video semantic segmentation of driving scenes. In *Proceedings of the IEEE/CVF Conference on Computer Vision and Pattern Recognition*, pages 3544–3553, 2024. 1
- [18] Ankit Gupta, Albert Gu, and Jonathan Berant. Diagonal state spaces are as effective as structured state spaces. *Advances in Neural Information Processing Systems*, 35:22982–22994, 2022. 3
- [19] Dongchen Han, Ziyi Wang, Zhuofan Xia, Yizeng Han, Yifan Pu, Chunjiang Ge, Jun Song, Shiji Song, Bo Zheng, and Gao Huang. Demystify mamba in vision: A linear attention perspective. *Advances in neural information processing systems*, 37:127181–127203, 2024. 3
- [20] Junjun He, Zhongying Deng, and Yu Qiao. Dynamic multi-scale filters for semantic segmentation. In *Proceedings of the IEEE/CVF international conference on computer vision*, pages 3562–3572, 2019. 1
- [21] Junjun He, Zhongying Deng, Lei Zhou, Yali Wang, and Yu Qiao. Adaptive pyramid context network for semantic segmentation. In *Proceedings of the IEEE/CVF conference on computer vision and pattern recognition*, pages 7519–7528, 2019. 1
- [22] Syed Ariff Syed Hesham, Yun Liu, Guolei Sun, Henghui Ding, Jing Yang, Ender Konukoglu, Xue Geng, and Xudong Jiang. Exploiting temporal state space sharing for video semantic segmentation. In *Proceedings of the Computer Vision and Pattern Recognition Conference*, pages 24211–24221, 2025. 2, 3, 4, 6, 7, 8
- [23] Ping Hu, Fabian Caba, Oliver Wang, Zhe Lin, Stan Sclaroff, and Federico Perazzi. Temporally distributed networks for fast video semantic segmentation. In *Proceedings of*

- the *IEEE/CVF conference on computer vision and pattern recognition*, pages 8818–8827, 2020. 2, 3
- [24] Samvit Jain, Xin Wang, and Joseph E Gonzalez. Accel: A corrective fusion network for efficient semantic segmentation on video. In *Proceedings of the IEEE/CVF Conference on Computer Vision and Pattern Recognition*, pages 8866–8875, 2019. 2
- [25] Angelos Katharopoulos, Apoorv Vyas, Nikolaos Pappas, and François Fleuret. Transformers are rnns: Fast autoregressive transformers with linear attention. In *International conference on machine learning*, pages 5156–5165. PMLR, 2020. 3
- [26] Jiangwei Lao, Weixiang Hong, Xin Guo, Yingying Zhang, Jian Wang, Jingdong Chen, and Wei Chu. Simultaneously short-and long-term temporal modeling for semi-supervised video semantic segmentation. In *Proceedings of the IEEE/CVF Conference on Computer Vision and Pattern Recognition*, pages 14763–14772, 2023. 2
- [27] Shih-Po Lee, Si-Cun Chen, and Wen-Hsiao Peng. Gsvnet: Guided spatially-varying convolution for fast semantic segmentation on video. *arXiv preprint arXiv:2103.08834*, 2021. 2
- [28] Jiangtong Li, Wentao Wang, Junjie Chen, Li Niu, Jianlou Si, Chen Qian, and Liqing Zhang. Video semantic segmentation via sparse temporal transformer. In *Proceedings of the 29th ACM International Conference on Multimedia*, pages 59–68, 2021. 2, 3
- [29] Kunchang Li, Xinhao Li, Yi Wang, Yinan He, Yali Wang, Limin Wang, and Yu Qiao. Videomamba: State space model for efficient video understanding. In *European Conference on Computer Vision*, pages 237–255. Springer, 2024. 2, 3
- [30] Qiwei Li, Kunlun Xu, Yuxin Peng, and Jiahuan Zhou. Exemplar-free lifelong person re-identification via prompt-guided adaptive knowledge consolidation. *International Journal of Computer Vision*, pages 1–16, 2024. 1
- [31] Yule Li, Jianping Shi, and Dahua Lin. Low-latency video semantic segmentation. In *Proceedings of the IEEE conference on Computer Vision and Pattern Recognition*, pages 5997–6005, 2018. 2
- [32] Yifan Liu, Chunhua Shen, Changqian Yu, and Jingdong Wang. Efficient semantic video segmentation with per-frame inference. In *European Conference on Computer Vision*, pages 352–368. Springer, 2020. 2
- [33] Yue Liu, Yunjie Tian, Yuzhong Zhao, Hongtian Yu, Lingxi Xie, Yaowei Wang, Qixiang Ye, Jianbin Jiao, and Yunfan Liu. Vmamba: Visual state space model. *Advances in neural information processing systems*, 37:103031–103063, 2024. 3
- [34] Ze Liu, Yutong Lin, Yue Cao, Han Hu, Yixuan Wei, Zheng Zhang, Stephen Lin, and Baining Guo. Swin transformer: Hierarchical vision transformer using shifted windows. In *Proceedings of the IEEE/CVF international conference on computer vision*, pages 10012–10022, 2021. 7
- [35] Hui Lu, Albert A Salah, and Ronald Poppe. Snakes and ladders: Two steps up for videomamba. In *Proceedings of the IEEE/CVF International Conference on Computer Vision*, pages 24234–24244, 2025. 3
- [36] Jun Ma, Feifei Li, and Bo Wang. U-mamba: Enhancing long-range dependency for biomedical image segmentation. *arXiv preprint arXiv:2401.04722*, 2024. 3
- [37] Jiaxu Miao, Yunchao Wei, Yu Wu, Chen Liang, Guangrui Li, and Yi Yang. Vspw: A large-scale dataset for video scene parsing in the wild. In *Proceedings of the IEEE/CVF conference on computer vision and pattern recognition*, pages 4133–4143, 2021. 6, 7, 8
- [38] David Nilsson and Cristian Sminchisescu. Semantic video segmentation by gated recurrent flow propagation. In *Proceedings of the IEEE conference on computer vision and pattern recognition*, pages 6819–6828, 2018. 1
- [39] Jinyoung Park, Hee-Seon Kim, Kangwook Ko, Minbeom Kim, and Changick Kim. Videomamba: Spatio-temporal selective state space model. In *European Conference on Computer Vision*, pages 1–18. Springer, 2024. 3
- [40] Matthieu Paul, Christoph Mayer, Luc Van Gool, and Radu Timofte. Efficient video semantic segmentation with labels propagation and refinement. In *Proceedings of the IEEE/CVF Winter Conference on Applications of Computer Vision*, pages 2873–2882, 2020. 2
- [41] Matthieu Paul, Martin Danelljan, Luc Van Gool, and Radu Timofte. Local memory attention for fast video semantic segmentation. In *2021 IEEE/RSJ International Conference on Intelligent Robots and Systems (IROS)*, pages 1102–1109. IEEE, 2021. 3
- [42] Andreas Pfeuffer, Karina Schulz, and Klaus Dietmayer. Semantic segmentation of video sequences with convolutional lstms. In *2019 IEEE intelligent vehicles symposium (IV)*, pages 1441–1447. IEEE, 2019. 2
- [43] Sébastien Piérard, Anthony Cioppa, Anaïs Halin, Renaud Vandeghen, Maxime Zanella, Benoît Macq, Saïd Mahmoudi, and Marc Van Droogenbroeck. Mixture domain adaptation to improve semantic segmentation in real-world surveillance. In *Proceedings of the IEEE/CVF Winter Conference on Applications of Computer Vision*, pages 22–31, 2023. 1
- [44] Rui Qian, Weiyao Lin, John See, and Dian Li. Controllable augmentations for video representation learning. *Visual Intelligence*, 2(1):1, 2024. 1
- [45] Laura Sevilla-Lara, Deqing Sun, Varun Jampani, and Michael J Black. Optical flow with semantic segmentation and localized layers. In *Proceedings of the IEEE conference on computer vision and pattern recognition*, pages 3889–3898, 2016. 1
- [46] Evan Shelhamer, Kate Rakelly, Judy Hoffman, and Trevor Darrell. Clockwork convnets for video semantic segmentation. In *European Conference on Computer Vision*, pages 852–868. Springer, 2016. 2
- [47] Evan Shelhamer, Jonathan Long, and Trevor Darrell. Fully convolutional networks for semantic segmentation. *IEEE Transactions on Pattern Analysis & Machine Intelligence*, 39(04):640–651, 2017. 2
- [48] Zhuoran Shen, Mingyuan Zhang, Haiyu Zhao, Shuai Yi, and Hongsheng Li. Efficient attention: Attention with linear complexities. In *Proceedings of the IEEE/CVF winter conference on applications of computer vision*, pages 3531–3539, 2021. 3

- [49] Xingjian Shi, Zhourong Chen, Hao Wang, Dit-Yan Yeung, Wai-Kin Wong, and Wang-chun Woo. Convolutional lstm network: A machine learning approach for precipitation nowcasting. *Advances in neural information processing systems*, 28, 2015. 2
- [50] Mennatullah Siam, Mostafa Gamal, Moemen Abdel-Razek, Senthil Yogamani, Martin Jagersand, and Hong Zhang. A comparative study of real-time semantic segmentation for autonomous driving. In *Proceedings of the IEEE conference on computer vision and pattern recognition workshops*, pages 587–597, 2018. 1
- [51] Mennatullah Siam, Alex Kendall, and Martin Jagersand. Video class agnostic segmentation benchmark for autonomous driving. In *Proceedings of the IEEE/CVF Conference on Computer Vision and Pattern Recognition*, pages 2825–2834, 2021. 1
- [52] Nathan Silberman, Derek Hoiem, Pushmeet Kohli, and Rob Fergus. Indoor segmentation and support inference from rgbd images. In *European conference on computer vision*, pages 746–760. Springer, 2012. 6, 7
- [53] Guolei Sun, Yun Liu, Henghui Ding, Thomas Probst, and Luc Van Gool. Coarse-to-fine feature mining for video semantic segmentation. In *proceedings of the IEEE/CVF conference on computer vision and pattern recognition*, pages 3126–3137, 2022. 2, 3, 7
- [54] Guolei Sun, Yun Liu, Hao Tang, Ajad Chhatkuli, Le Zhang, and Luc Van Gool. Mining relations among cross-frame affinities for video semantic segmentation. In *European Conference on Computer Vision*, pages 522–539. Springer, 2022. 3, 6, 7
- [55] Guolei Sun, Yun Liu, Henghui Ding, Min Wu, and Luc Van Gool. Learning local and global temporal contexts for video semantic segmentation. *IEEE Transactions on Pattern Analysis and Machine Intelligence*, 46(10):6919–6934, 2024. 2, 6, 7, 8
- [56] Ashish Vaswani, Noam Shazeer, Niki Parmar, Jakob Uszkoreit, Llion Jones, Aidan N Gomez, Lukasz Kaiser, and Illia Polosukhin. Attention is all you need. *Advances in neural information processing systems*, 30, 2017. 3
- [57] Roger Waleffe, Wonmin Byeon, Duncan Riach, Brandon Norick, Vijay Korthikanti, Tri Dao, Albert Gu, Ali Hatamizadeh, Sudhakar Singh, Deepak Narayanan, et al. An empirical study of mamba-based language models. *arXiv preprint arXiv:2406.07887*, 2024. 3
- [58] Sinong Wang, Belinda Z Li, Madian Khabsa, Han Fang, and Hao Ma. Linformer: Self-attention with linear complexity. *arXiv preprint arXiv:2006.04768*, 2020. 3
- [59] Yuetian Weng, Mingfei Han, Haoyu He, Mingjie Li, Lina Yao, Xiaojun Chang, and Bohan Zhuang. Mask propagation for efficient video semantic segmentation. *Advances in Neural Information Processing Systems*, 36:7170–7183, 2023. 3, 6
- [60] Chaodong Xiao, Minghan Li, Zhengqiang Zhang, Deyu Meng, and Lei Zhang. Spatial-mamba: Effective visual state space models via structure-aware state fusion. In *The Thirteenth International Conference on Learning Representations*, 2025. 3
- [61] Enze Xie, Wenhai Wang, Zhiding Yu, Anima Anandkumar, Jose M Alvarez, and Ping Luo. Segformer: Simple and efficient design for semantic segmentation with transformers. *Advances in neural information processing systems*, 34: 12077–12090, 2021. 3, 6, 7
- [62] Kunlun Xu, Haozhuo Zhang, Yu Li, Yuxin Peng, and Jiahuan Zhou. Mitigate catastrophic remembering via continual knowledge purification for noisy lifelong person re-identification. In *Proceedings of the 32nd ACM International Conference on Multimedia*, pages 5790–5799, 2024. 1
- [63] Kunlun Xu, Xu Zou, Yuxin Peng, and Jiahuan Zhou. Distribution-aware knowledge prototyping for non-exemplar lifelong person re-identification. In *Proceedings of the IEEE/CVF Conference on Computer Vision and Pattern Recognition*, pages 16604–16613, 2024.
- [64] Kunlun Xu, Xu Zou, and Jiahuan Zhou. Lstkc: Long short-term knowledge consolidation for lifelong person re-identification. In *Proceedings of the AAAI Conference on Artificial Intelligence*, pages 16202–16210, 2024.
- [65] Kunlun Xu, Chenghao Jiang, Peixi Xiong, Yuxin Peng, and Jiahuan Zhou. Dask: Distribution rehearsing via adaptive style kernel learning for exemplar-free lifelong person re-identification. In *Proceedings of the AAAI Conference on Artificial Intelligence*, pages 8915–8923, 2025.
- [66] Kunlun Xu, Zichen Liu, Xu Zou, Yuxin Peng, and Jiahuan Zhou. Long short-term knowledge decomposition and consolidation for lifelong person re-identification. *IEEE Transactions on Pattern Analysis and Machine Intelligence*, 2025.
- [67] Kunlun Xu, Fan Zhuo, Jiangmeng Li, Xu Zou, and Jiahuan Zhou. Self-reinforcing prototype evolution with dual-knowledge cooperation for semi-supervised lifelong person re-identification. In *Proceedings of the IEEE/CVF International Conference on Computer Vision*, pages 3564–3574, 2025.
- [68] Kunlun Xu, Xu Zou, Gang Hua, and Jiahuan Zhou. Componential prompt-knowledge alignment for domain incremental learning. In *International Conference on Machine Learning*, pages 70032–70046. PMLR, 2025. 1
- [69] Xiaolong Xu, Lei Zhang, Jiayi Li, Lituan Wang, Yifan Guan, Yu Yan, Leyi Zhang, and Hao Song. Dual-temporal exemplar representation network for video semantic segmentation. In *Proceedings of the IEEE/CVF International Conference on Computer Vision*, pages 10775–10785, 2025. 3
- [70] Yiran Xu, Badour AlBahar, and Jia-Bin Huang. Temporally consistent semantic video editing. In *European Conference on Computer Vision*, pages 357–374. Springer, 2022. 1
- [71] Yijun Yang, Zhaohu Xing, and Lei Zhu. Vivim: a video vision mamba for medical video object segmentation. *arXiv preprint arXiv:2401.14168*, 2024. 3
- [72] Zhifan Ye, Kejing Xia, Yonggan Fu, Xin Dong, Jihoon Hong, Xiangchi Yuan, Shizhe Diao, Jan Kautz, Pavlo Molchanov, and Yingyan Celine Lin. Longmamba: Enhancing mamba’s long context capabilities via training-free receptive field enlargement. *arXiv preprint arXiv:2504.16053*, 2025. 3
- [73] Weihao Yu and Xinchao Wang. Mambaout: Do we really need mamba for vision? In *Proceedings of the Computer Vision and Pattern Recognition Conference*, pages 4484–4496, 2025. 3

- [74] Jiahuan Zhou, Kunlun Xu, Fan Zhuo, Xu Zou, and Yuxin Peng. Distribution-aware knowledge aligning and prototyping for non-exemplar lifelong person re-identification. *IEEE Transactions on Pattern Analysis and Machine Intelligence*, 2025. 1
- [75] Jiahuan Zhou, Kai Zhu, Zhenyu Cui, Zichen Liu, Xu Zou, and Gang Hua. State space prompting via gathering and spreading spatio-temporal information for video understanding. In *The Thirty-ninth Annual Conference on Neural Information Processing Systems*, 2025. 3
- [76] Lianghai Zhu, Bencheng Liao, Qian Zhang, Xinlong Wang, Wenyu Liu, and Xinggang Wang. Vision mamba: Efficient visual representation learning with bidirectional state space model. In *Forty-first International Conference on Machine Learning*, 2024. 3
- [77] Xizhou Zhu, Yuwen Xiong, Jifeng Dai, Lu Yuan, and Yichen Wei. Deep feature flow for video recognition. In *Proceedings of the IEEE conference on computer vision and pattern recognition*, pages 2349–2358, 2017. 2
- [78] Itamar Zimmerman, Ameen Ali Ali, and Lior Wolf. Explaining modern gated-linear RNNs via a unified implicit attention formulation. In *The Thirteenth International Conference on Learning Representations*, 2025. 3